Key Role of the Cation Interstitial Structure in the Radiation Resistance of Pyrochlores

Alain Chartier,[1] Gilles Catillon,[2] and Jean-Paul Crocombette[3]
[1]CEA Saclay, SCP, F-91191 Gif-sur-Yvette, France
[2]Université Paris-Est, G2I, EA 4119, 5 Boulevard Descartes, F-77454 Marne la Vallée cedex 2, France
[3]CEA Saclay, SRMP, F-91191 Gif-sur-Yvette, France
(Received 17 February 2009; published 15 April 2009)

The annealing of the B cation interstitial is shown to drive the thermokinetic of the response to irradiations of $A_2B_2O_7$ pyrochlores. Molecular dynamics simulations evidenced that the annealing of interstitials created by irradiations depends upon the nature of B. As the coordination number of B decreases, the dumbbell interstitial is stabilized at the expense of the isolated interstitial. Unlike the isolated interstitials, the recombination of the dumbbells is thermally activated and hindered at low temperatures. The occurrence of dumbbells drives the structure towards the amorphous state.

DOI: 10.1103/PhysRevLett.102.155503 PACS numbers: 61.80.−x, 61.43.Bn, 64.60.−i

Among the structurally related fluorite compounds, the pyrochlore oxides ($A_2B_2O_7$) have many technological applications due to the variety of their properties [1–3]. A fundamental understanding of their response to irradiations is also of utmost interest for the nuclear industry as they can be used as an inert matrix [2]. We focus here on the $Gd_2Zr_xTi_{2-x}O_7$ ($0 \leq x \leq 2$) solid solution as it is a textbook example of the response of pyrochlores under irradiations [2]. Its response varies widely with composition [4], from no amorphization in $Gd_2Zr_2O_7$ at any temperature (down to 30 K) to complete amorphization in $Gd_2Ti_2O_7$ up to a so-called critical temperature, beyond which no amorphization is possible.

The current understanding of the variation of the radiation resistance in the pyrochlore family is based on the Subramanian *et al.* [5] criterion: the closer the ionic radii of cations A and B (in $A_2B_2O_7$), the lower the energy difference between the ordered pyrochlore and the corresponding disordered fluorite structure and consequently the more radiation resistant is the pyrochlore. The ionic radius ratio between A and B has been related to the formation energy [6,7] and to the antisite (AS) energy [8] of the pyrochlores.

The relative radiation resistance of two pyrochlore compositions can thus be inferred from comparison of the respective values of any of the aforementioned quantities. However, all of them are ground state properties while stability under irradiation obviously relates to a nonequilibrium phenomenon. Indeed steady states under irradiations come from the balance between the disordering caused by irradiations and the dynamical annealing (which can be either thermal or irradiation induced) as expressed in the form of phenomenological rate equations [9].

As cascades create only point defects in pyrochlore [10–13], one traditionally calls upon some long range diffusion of point defects for the annealing phenomenon [1]. Unfortunately, the measured activation energies that appear in the rate equations are by far too small to be related to any diffusion process. Recent studies in the $La_2Zr_2O_7$ pyrochlore [14–17] have advocated that the thermally activated recombination of close cation interstitial-vacancy (Frenkel) pairs can be the healing process.

In this Letter, we show that continuous Frenkel pairs' (FP) accumulation within molecular dynamics (MD) [16] can quantitatively reproduce the irradiation response of the whole solid solution $Gd_2Zr_xTi_{2-x}O_7$, as a function of composition and temperature. The decrease of the radiation resistance as a function of the increase of Ti content in $Gd_2Zr_xTi_{2-x}O_7$ is shown to be driven by a change in the configuration of the B interstitials. In fact, the stabilization of Ti-Ti dumbbells in the partially disordered fluorite structure hinders their recombination with vacancies. Conversely, the isolated Zr interstitials readily recombine with vacancies. So, as the amount of Ti increases in the B site of $Gd_2B_2O_7$, the stability of the B-B dumbbells increases in the fluorite structure and prevents the reconstruction of the structure which eventually collapses to the amorphous state. Present calculations also unify the previous ground states based criteria [5–8] and introduce the recombination of the B-B dumbbells as the missing phenomenon in the rate equations [9].

We have used in the present work the Buckingham potentials established by Purton and Allan [10–12] for the description of the $Gd_2Zr_xTi_{2-x}O_7$ solid solution. Using methods detailed in previous papers [16,17], the physical properties of fluorite and amorphous structures were calculated for $Gd_2Ti_2O_7$ and $Gd_2Zr_2O_7$. The results reported Table I indicate that these potentials are reliable for the investigation of the phase transition of $Gd_2Zr_xTi_{2-x}O_7$ under irradiations.

As displacement cascades produce only point defects, one can mimic the effect of cascade accumulation by the continuous accumulation of Frenkel pairs (see [16] for details). We have considered the same five compositions as in experiments: $Gd_2Zr_2O_7$, $Gd_2Zr_{1.5}Ti_{0.5}O_7$, Gd_2ZrTiO_7, $Gd_2Zr_{0.5}Ti_{1.5}O_7$, and $Gd_2Ti_2O_7$. For the intermediate compositions, the Zr and Ti cations were randomly distributed in the B sublattices. Cation Frenkel pairs were then randomly introduced one after the other

TABLE I. Calculated properties of $Gd_2Zr_2O_7$ (GZ) and $Gd_2Ti_2O_7$ (GT). *P*, *F*, and *A* stand for pyrochlore, fluorite, and amorphous structures, respectively. CN stands for coordination number. $\Delta E_B(D\text{-}I)$ stands for the energy difference between the isolated *B* interstitial (*I*) and *B*-*B* dumbbell (*D*) configurations in Gd or *B* site. A positive value indicates that the isolated interstitial is the more stable. ΔE_{AS} is the antisite formation energy (eV). ΔE is the energy difference of the *A* and *F* structure with respect to the *P* structure. Experiments give $\Delta E_{P\text{-}F}(Gd_2Zr_2O_7) = 0.104$ eV/atom [18].

			CN		$\Delta E_B(D\text{-}I)$		
		ΔE (eV/atom)	Gd	*B*	Gd_{site}	B_{site}	ΔE_{AS}
GT	*P*	0.000	8.0	6.0	−2.7	2.0	6.0
	F	0.368	7.2	6.4	−0.4		···
	A	0.353	6.3	5.7	···		···
GZ	*P*	0.000	8.0	6.0	3.4	1.2	2.6
	F	0.141	7.0	7.0	*D* unstable		···
	A	0.236	7.2	6.8	···		···

with a 1 ps interval between two subsequent FP creations. Only cation FPs were created, in light of previous results in the $La_2Zr_2O_7$ pyrochlore [15,17] which showed that the oxygen disorder is essentially driven by the disorder of cations. The dose of irradiation was consequently counted in displacement per cation (dpc).

We have reported in Fig. 1 the evolution of the amorphization dose *D* of $Gd_2Zr_xTi_{2-x}O_7$ as a function of temperature and composition. *D* is defined as the dose at which the vacancy concentration gets higher than 0.5 (see Fig. 4). One can see that under FP accumulation, $Gd_2Zr_xTi_{2-x}O_7$ shows an increase of the radiation resistance (increase of *D*, Fig. 1) as a function of the zirconium content *x* and as a function of temperature. Moreover, $Gd_2Zr_2O_7$ shows a complete transition towards the fluorite structure, but never collapses towards the amorphous state under FP accumulation (up to the highest calculated dose of 21.5 dpc). Conversely, $Gd_2Ti_2O_7$ always amorphizes before reaching the fully disordered fluorite structure. The

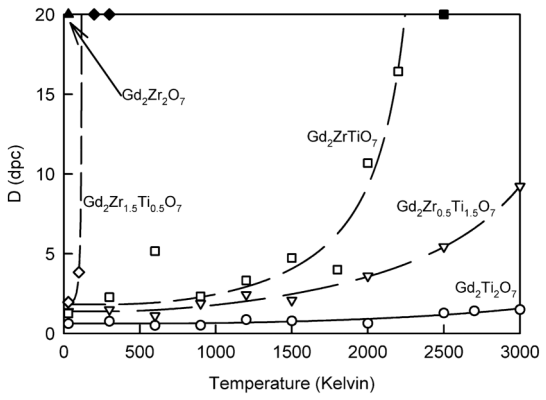

FIG. 1. Critical doses *D* (open symbols) for amorphization as a function of temperature. The lines represent the fits obtained using Eq. (1). Filled symbols represent the maximum doses at which no amorphization has been detected.

intermediate compositions $Gd_2Zr_{0.5}Ti_{1.5}O_7$, Gd_2ZrTiO_7, and $Gd_2Zr_{1.5}Ti_{0.5}O_7$ show intermediate behaviors between the end members. They first transit towards the disordered fluorite structure before the eventual amorphization which proves more and more difficult to achieve with increasing the zirconium content. These results perfectly reproduce the experimental observations [4,19,20].

Using phenomenological rate equations (after Weber [9]), which account for the balance between competing phenomena of disordering and annealing, we can fit the doses *D* for amorphization as a function of temperature *T* (see Fig. 1) with the following formula:

$$\ln\left(1 - \frac{D_0}{D}\right) = C - \frac{E_{act}}{k_B T}. \quad (1)$$

D_0 is the critical dose for amorphization extrapolated at 0 K, *C* is a constant independent of the irradiation flux, and E_{act} is the effective activation energy of the annealing term. The results have been reported as lines in Fig. 1, and the fitted parameters are in Table II. As may easily be seen, the critical temperatures T_C are very large. This relates to an irradiation flux effect. Indeed the rate of creation of disorder in the simulation (4×10^9 dpc/s) is much higher than the one of experiments (3.3×10^{-3} dpa/s with 1.0 MeV Kr^+ [4,19,20]). Assuming that the recovery processes are of thermal origin (as opposed to irradiation assisted) one can account for the flux effect in T_C using the following formula [9]:

$$T_C = \frac{E_{act}}{k_B \ln(C_{mater}/\Phi)}. \quad (2)$$

In this equation, C_{mater} is a constant characteristic of each material. It represents the ratio between annealing and damage cross sections and is independent of the irradiation flux Φ. Assuming a value of $C_{mater} = 2 \times 10^{13}$ dpc/s constant over the whole solid solution, T_C have been rescaled. The values corrected for the flux have been reported in Fig. 2. The critical temperature for amorphization T_C decreases as a function of the zirconium content in $Gd_2Zr_xTi_{2-x}O_7$ and is in excellent quantitative agreement with the experimental observations [4,19,20].

The very good agreement obtained with experiments proves that the recovery processes are indeed of thermal origin. It also indicates that these processes are active in the present simulations and therefore offer the opportunity to

TABLE II. Critical doses for amorphization D_0, effective activation energies E_{act}, and critical temperatures for amorphization T_C for $Gd_2Zr_xTi_{2-x}O_7$ obtained by the fits of the MD calculations with Eq. (1) and reported on Fig. 1.

x	D_0 (dpc)	E_{act} (eV)	T_C (Kelvin)
0.0	0.62	0.33	4944
0.5	1.37	0.17	3982
1.0	1.81	0.18	2480
1.5	1.96	0.03	122

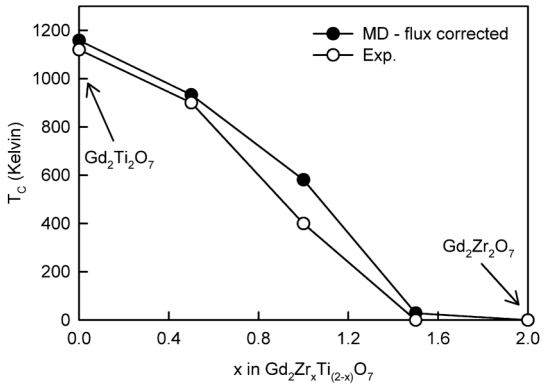

FIG. 2. Comparison between the MD flux corrected [using Eq. (2)] and the experimental evolution [4,19,20] of the critical temperatures of amorphization T_C.

identify the underlying mechanisms that drive the response of pyrochlores under irradiations. We focus on the FP accumulations in $Gd_2Zr_2O_7$ and $Gd_2Ti_2O_7$ at 30 K (Figs. 3 and 4) as they are generic to the whole $Gd_2Zr_xTi_{2-x}O_7$ solid solution.

We found that the variations in radiation resistance relate to the occurrence of two different configurations of the B (either Zr or Ti) interstitials. Upon FP accumulation Zr interstitial mainly remains in an isolated configuration (in the 32e site, and see Fig. 3). On the other hand, Ti interstitials exhibit a Ti-Ti dumbbell configuration which proves to have a quite different behavior from the usual isolated interstitial configuration (see Fig. 4).

Isolated interstitials are found to be prone to recombinations with the surrounding vacancies of any cationic type following the general patterns observed in fluorite structures [21,22]. These recombinations smoothly induce the formation of antisites and lead the material towards a disordered fluorite structure. On the other hand, Ti-Ti dumbbells prove much more difficult to recombine with vacancies. The stability of these Ti-Ti dumbbells leads to the accumulation of vacancies. Both vacancies and Ti-Ti dumbbells (see Fig. 4) eventually cause the collapse of the crystalline structure. Some structural disorder is needed to trigger the occurrence of such Ti-Ti dumbbell configurations. Indeed no such dumbbells are seen in the initial stages of the accumulation of defects because the stabilization of a Ti-Ti dumbbell configuration requires the preexistence of Ti AS.

The above observations are confirmed by the energy of formation of the interstitials (Table I). In fact, we have calculated that the dumbbell configuration of Zr interstitial has a higher energy than the isolated configuration in pyrochlore and is even mechanically unstable in fluorite. The energetic of the Ti-Ti dumbbell configuration is a little more complicated. It proves unfavorable in the B site but favorable in the AS (Gd site) of ordered pyrochlore (with respect to the isolated configuration). The Ti-Ti dumbbell is also favorable in the fluorite structure, but with a smaller energy difference (Table I). So a small amount of AS in ordered pyrochlore is sufficient to drive the stabilization of Ti-Ti dumbbells (see Fig. 4).

The formation energies of interstitials and AS may be related to the coordination number (CN) of B (either Zr or Ti), in the spirit of Reznitskii [23]. The isolated 32e interstitial sites (in both pyrochlore and fluorite structures)

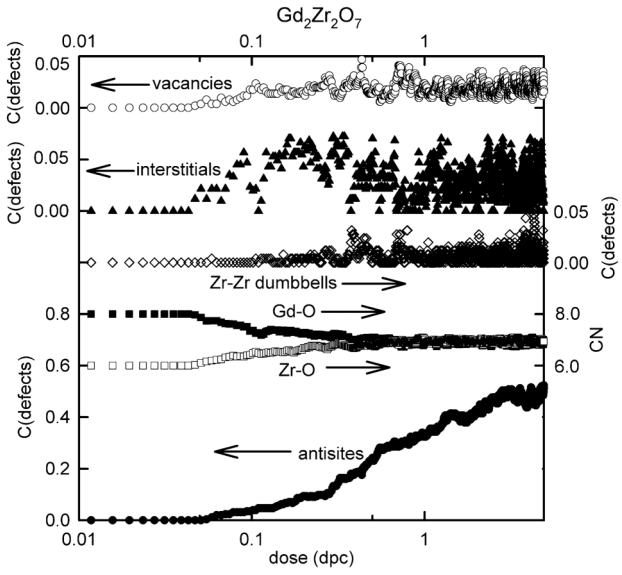

FIG. 3. Evolution of the concentrations of cation vacancies, interstitials, antisites, and Zr-Zr dumbbells quoted C(defects), and the coordination number (CN) as a function of the dose in dpc (displacement per cation) of $Gd_2Zr_2O_7$ at 30 K.

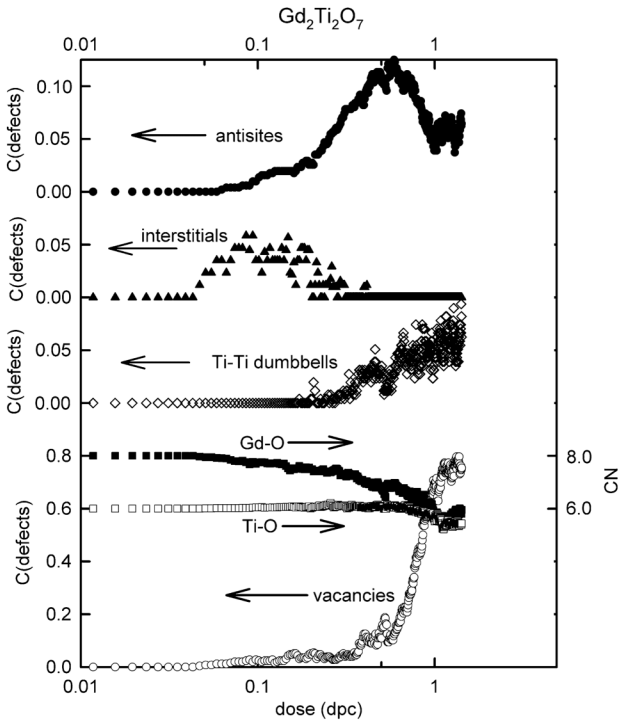

FIG. 4. Evolution of the concentrations of defects C(defects) and the CN as a function of the dose of $Gd_2Ti_2O_7$ at 30 K.

and the AS have a higher CN than the normal B site (respectively 7 and 8 for the 32e site and the AS). Such a high CN is easily accommodated by Zr in $Gd_2Zr_2O_7$ (see Table I and Fig. 3) as in monoclinic zirconia ZrO_2. Conversely, a high CN is hardly accommodated by Ti. This difference between Ti and Zr also appears in the higher formation energy of AS in $Gd_2Ti_2O_7$ than in $Gd_2Zr_2O_7$ (Table I). The formation of a Ti-Ti dumbbell causes a decrease of the CN to more favorable values of around 5. In fact, such Ti-Ti dumbbell configurations have been observed in amorphous TiO_2 (CN = 5.4 [24]), in metamict zirconolite and many amorphous pyrochlores [25,26]. Our calculations also exhibit these dumbbell structures in amorphous $Gd_2Ti_2O_7$ (Table I and Fig. 4).

The change in the facility to recombine the B interstitials with first neighbor vacancies when comparing the isolated and dumbbell configurations drives the change in the amorphization resistance in the $Gd_2Zr_xTi_{2-x}O_7$ series. To evidence this proposition, we recall that isolated interstitials of any type (either Ti, Zr, or Gd) spontaneously recombine with first neighbor vacancies. On the other hand, we have performed static calculations that show that the recombination of the Ti-Ti dumbbell with a first neighbor vacancy is thermally activated. The calculated activation energy is 0.25 eV, which is close to 0.33 eV obtained for the critical dose for amorphization (see Table II).

The present results bring some generic insights on the radiation resistance of pyrochlores. As said above, the ground state criteria used to classify the radiation resistance of various pyrochlores eventually relate to ionic radius ratio considerations [3–8,27]. The embodiment of the ionic radius change in the context of irradiation is the change of stability of the two kinds of configuration of the cationic interstitials. This change has been discussed above in term of preferential cationic coordination number which is directly piloted by the value of the ionic radius as expressed by Pauling's rule.

The present results are thus consistent with the ground state criteria but also relate these criteria to a characteristic specific to irradiation, namely, the configuration of interstitials, and add the missing mechanism for annealing. Indeed the thermally activated recombinations of the vacancy-interstitial first neighbor pairs pilot the variable radiation resistance of $A_2B_2O_7$ as a function of temperature and composition.

Computing facilities were provided by CINES (Project No. ggi2757) and CCRT. G. C. would like to thank A. Mango and J.-L. Ambrosino from CINES for their help.

[1] S. Hull, Rep. Prog. Phys. **67**, 1233 (2004).
[2] R. C. Ewing, W. J. Weber, and J. Lian, J. Appl. Phys. **95**, 5949 (2004).
[3] J. Lian, L. M. Wang, S. X. Wang, J. Chen, L. A. Boatner, and R. C. Ewing, Phys. Rev. Lett. **87**, 145901 (2001).
[4] S. X. Wang, B. D. Begg, L. M. Wang, R. C. Ewing, W. J. Weber, and K. V. Govidan Kutty, J. Mater. Res. **14**, 4470 (1999).
[5] M. A. Subramanian, G. Aravamudan, and C. V. Subbs Rao, Prog. Solid State Chem. **15**, 55 (1983).
[6] K. B. Helean, S. V. Ushakov, C. E. Brown, A. Navrotsky, J. Lian, R. C. Ewing, J. M. Farmer, and L. A. Boatner, J. Solid State Chem. **177**, 1858 (2004).
[7] K. E. Sickafus, R. W. Grimes, J. A. Valdez, A. Cleave, M. Tang, M. Ishimaru, S. M. Corish, C. R. Stanek, and B. P. Uberuaga, Nature Mater. **6**, 217 (2007).
[8] K. E. Sickafus, L. Minervini, R. W. Grimes, J. A. V. Ishimaru, F. Li, K. J. McLellan, and T. Hartmann, Science **289**, 748 (2000).
[9] W. J. Weber, Nucl. Instrum. Methods Phys. Res., Sect. B **166–167**, 98 (2000).
[10] J. A. Purton and N. L. Allan, J. Mater. Chem. **12**, 2923 (2002). The Buckingham parameter A(Gd-O) has been changed to 4561.9633 eV.
[11] I. T. Todorov, J. A. Purton, N. L. Allan, and M. T. Dove, J. Phys. Condens. Matter **18**, 2217 (2006).
[12] I. T. Todorov, N. L. Allan, J. A. Purton, M. T. Dove, and W. Smith, J. Mater. Sci. **42**, 1920 (2007).
[13] R. Devanathan and W. J. Weber, J. Appl. Phys. **98**, 086110 (2005).
[14] A. Chartier, C. Meis, J.-P. Crocombette, L. R. Corrales, and W. J. Weber, Phys. Rev. B **67**, 174102 (2003).
[15] A. Chartier, C. Meis, J.-P. Crocombette, W. J. Weber, and L. R. Corrales, Phys. Rev. Lett. **94**, 025505 (2005).
[16] J.-P. Crocombette, A. Chartier, and W. J. Weber, Appl. Phys. Lett. **88**, 051912 (2006).
[17] J.-P. Crocombette and A. Chartier, Nucl. Instrum. Methods Phys. Res., Sect. B **255**, 158 (2007).
[18] K. B. Helean, B. D. Begg, A. Navrotsky, B. Ebbinghaus, W. J. Weber, and R. C. Ewing, in *Scientific Basis for Nuclear Waste Management XXIV*, MRS Proc. No. 663 Materials Research Society, Warrendale, PA, 2001, p. 691.
[19] J. Lian, L. M. Wang, J. Chen, R. C. Ewing, and K. V. Govidan Kutty, in *Scientific Basis for Nuclear Waste Management XXV*, MRS Proc. No. 713 (Materials Research Society, Warrendale, PA, 2001), p. JJ11.35.
[20] J. Lian, J. Chen, L. M. Wang, R. C. Ewing, J. M. Farmer, L. A. Boatner, and K. B. Helean, Phys. Rev. B **68**, 134107 (2003).
[21] L. Van Brutzel, A. Chartier, and J.-P. Crocombette, Phys. Rev. B **78**, 024111 (2008).
[22] A. Guglielmetti, A. Chartier, L. Van Brutzel, J.-P. Crocombette, K. Yasuda, C. Meis, and S. Matsumura, Nucl. Instrum. Methods Phys. Res., Sect. B **266**, 5120 (2008).
[23] L. A. Reznitskii, Inorg. Mater. **29**, 1166 (1993).
[24] V. Petkov, G. Holhüter, U. Tröge, Th. Gerber, and B. Himmel, J. Non-Cryst. Solids **231**, 17 (1998).
[25] F. Farges, Am. Mineral. **82**, 44 (1997).
[26] F. Farges, G. E. Brown, Jr., and J. J. Rehr, Phys. Rev. B **56**, 1809 (1997).
[27] G. R. Lumpkin, M. Pruneda, S. Rios, K. L. Smith, K. Trachenko, K. R. Whittle, and N. J. Zaluzec, J. Solid State Chem. **180**, 1512 (2007).